

STABILIZED WEIGHTED REDUCED BASIS METHODS FOR PARAMETRIZED ADVECTION DOMINATED PROBLEMS WITH RANDOM INPUTS [‡]

DAVIDE TORLO ^{*†}, FRANCESCO BALLARIN^{*}, AND GIANLUIGI ROZZA^{*}

Abstract. In this work, we propose viable and efficient strategies for stabilized parametrized advection dominated problems, with random inputs. In particular, we investigate the combination of wRB (weighted reduced basis) method for stochastic parametrized problems with stabilized reduced basis method, which is the integration of classical stabilization methods (SUPG, in our case) in the Offline–Online structure of the RB method. Moreover, we introduce a reduction method that selectively enables online stabilization; this leads to a sensible reduction of computational costs, while keeping a very good accuracy with respect to high fidelity solutions. We present numerical test cases to assess the performance of the proposed methods in steady and unsteady problems related to heat transfer phenomena.

Key words. random inputs, reduced basis methods, uncertainty quantification, stochastic parametrized advection diffusion equations, advection dominated problems.

AMS subject classifications. 35J15, 65C30, 65N35, 60H15, 60H35

1. Introduction. Advection–diffusion equations are very important in many engineering applications, because they are used to model, for example, heat transfer phenomena [25] or the diffusion phenomena, such as of pollutants in the atmosphere [12]. We are interested in studying related advection–diffusion PDEs when their Péclet numbers, representing, roughly, the ratio between the advection and the diffusion field, are high. Moreover, in such applications, we often need very fast evaluations of the approximated solution, depending on some input parameters, which may be deterministic or uncertain. This happens, for example, in the case of *real-time* simulation or if we need to perform repeated approximations of solutions, for different input parameters. We find such *many-query* situations in optimization problems, in which the objective function to be optimized depends on the parameters through the solution of a PDE or a system of PDEs.

The aim of this work is to study a stabilized reduced basis method suitable for the approximation of parametrized advection–diffusion partial differential equations (PDEs), in advection dominated cases, including a stochastic context, by considering random inputs. Indeed, the reduced basis (RB) method [20] has been devised to reduce the computational effort required by the repeated solution of parametrized problems. It provides rapidly approximation of solution of PDEs and it is able to guarantee the *reliability* of the solution with a sharp and accurate *a posteriori* error bound. In literature we can find many works about the application of the RB method to advection–diffusion problems, in particular with low Péclet number [16, 40, 44].

In contrast, problems characterized by high Péclet numbers are far more complex and may exhibit instabilities even with classical high fidelity numerical approximations, such as finite element or finite difference method. To deal with this issue we have to resort to some stabilization techniques [7, 42], such as SUPG stabilization. A similar stabilization needs to be accounted for also at the reduced order level, resulting in a stabilized version of the RB algorithm [37, 38, 39]. In particular, in these works it was shown that a double stabilization in *Offline* and *Online* stage was necessary to obtain an accurate approximation. Nevertheless, stabilizations in *Online* phase can be a bothersome computational cost that may damage the efficiency of the method (for example in *many-query* context), while in some other situation an *Offline-only* stabilized method can be

[‡]Submitted to the editors in September 2017.

Funding: This work was funded by European Union Funding for Research and Innovation (project H2020 ERC CoG 2015 AROMA-CFD project 681447) and by the INDAM-GNCS project.

^{*}mathLab, Mathematics Area, SISSA, Via Bonomea 265, I-34136 Trieste, Italy

[†]Current address: Institut für Mathematik. UZH, Universität Zürich, Winterthurerstrasse 190, CH-8057, Zürich, Switzerland

preferred. Stabilization of problems characterized by strong convection effects is an active topic of research in the model order reduction community, see e.g. [1, 2, 3, 13, 17, 23, 24, 31, 32, 37, 38, 45] for several different proposed methods with applications in heat transfer and computational fluid dynamics.

When dealing with stochastic equations, i.e., with random input parameters, we can modify the RB method, according to probability laws that rule our parameters. In this direction, the wRB (weighted reduced basis) method [9] wants to exploit all the information that random variables give us (a review is provided in [11]). In particular, we will apply it to stabilized reduced basis strategies and prove the accuracy of this combined method. Throughout the work we will test these methods on some steady and time-dependent problems.

The outline of the manuscript is as follows. In section 2 we will briefly introduce elliptic coercive parametrized PDEs, their associate RB method, some classical stabilization methods for FE approximation of advection dominated problems; then we will study two reduced basis stabilization methods by testing them on some examples. We will consider next stochastic partial differential equations; we will present in section 3 the weighted RB method and we will combine it with proper stabilization techniques. Moreover, we will provide a method that selectively enables stabilization to optimize computational costs. In section 4 we will extend these ideas to parabolic problems, by introducing the general weighted RB method for these problems, combining it with a suitable stabilization technique (based on stabilization for the FE approximation of advection dominated parabolic problems), and testing it on few examples. Finally, section 5 will provide some conclusions and future perspectives.

2. Stabilized reduced basis method for elliptic equations.

2.1. A brief introduction to reduced basis method. The reduced basis (RB) method is a reduced order modelling (ROM) technique which provides rapid and reliable solutions for parametrized partial differential equations (PPDEs) [20], in which the parameters can be either physical or geometrical, deterministic or stochastic.

The need to solve this kind of problems arises in many engineering applications, in which the evaluation of some *output* quantities is required. These *outputs* are often functionals of the solution of a PDE, which can in turn depend on some *input* parameters. The aim of the RB method is to provide a very fast computation of this *input-output* evaluation and so it turns out to be very useful especially in *real-time* or *many-query* contexts.

Roughly speaking, given a value of the parameter, the (Lagrange) RB method consists in a Galerkin projection of the continuous solution on a particular subspace of a high-fidelity approximation space, e.g. a finite element (FE) space with a large number of degrees of freedom. This subspace is the one spanned by some pre-computed high-fidelity global solutions (snapshots) of the continuous parametrized problem, corresponding to some properly chosen values of the parameter.

For a complete presentation of the reduced basis method we refer to [20], now we just recall its main features in order to introduce some notations.

2.1.1. The continuous problem. Let $\boldsymbol{\mu}$ belong to the parameter domain $\mathcal{D} \subset \mathbb{R}^p$. Let Ω be a regular bounded open subset of \mathbb{R}^d , ($d = 1, 2, 3$) and X a suitable Hilbert space. Given a parameter value $\boldsymbol{\mu} \in \mathcal{D}$, let $a(\cdot, \cdot; \boldsymbol{\mu}) : X \times X \rightarrow \mathbb{R}$ be a bilinear form and let $F(\cdot; \boldsymbol{\mu}) : X \rightarrow \mathbb{R}$ be a linear functional. As we will focus on advection-diffusion equations, that are second order elliptic PDE, the space X will be such that $H_0^1(\Omega) \subset X \subset H^1(\Omega)$. Formally, our problem can be written as follows:

$$(1) \quad \begin{aligned} &\text{find } u(\boldsymbol{\mu}) \in X : \\ &a(u(\boldsymbol{\mu}), v; \boldsymbol{\mu}) = F(v; \boldsymbol{\mu}), \quad \forall v \in X. \end{aligned}$$

We require a to be coercive and continuous, i.e., respectively:

$$(2) \quad \exists \alpha_0 \text{ s.t. } \alpha_0 \leq \alpha(\boldsymbol{\mu}) = \inf_{v \in X} \frac{a(v, v; \boldsymbol{\mu})}{\|v\|_X^2}, \quad \forall \boldsymbol{\mu} \in \mathcal{D},$$

and

$$(3) \quad +\infty > \gamma(\boldsymbol{\mu}) = \sup_{v \in X} \sup_{w \in X} \frac{|a(v, w; \boldsymbol{\mu})|}{\|v\|_X \|w\|_X}, \quad \forall \boldsymbol{\mu} \in \mathcal{D}.$$

For the sake of online efficiency, we assume an *affine* dependence of a on the parameter $\boldsymbol{\mu}$, i.e. we assume that

$$(4) \quad a(v, w; \boldsymbol{\mu}) = \sum_{q=1}^{Q_a} \Theta_a^q(\boldsymbol{\mu}) a^q(v, w), \quad \forall \boldsymbol{\mu} \in \mathcal{D}.$$

Here, $\Theta_a^q(\boldsymbol{\mu}) : \mathcal{D} \rightarrow \mathbb{R}$, $q = 1, \dots, Q_a$, are smooth functions, while $a^q : X \times X \rightarrow \mathbb{R}$, $q = 1, \dots, Q_a$, are $\boldsymbol{\mu}$ -independent continuous bilinear forms.

In a similar way, we assume that also the functional F is continuous and depends “affinely” on parameters:

$$(5) \quad F(v; \boldsymbol{\mu}) = \sum_{q=1}^{Q_F} \Theta_F^q(\boldsymbol{\mu}) F^q(v), \quad \forall \boldsymbol{\mu} \in \mathcal{D},$$

where, also in this case, $\Theta_F^q(\boldsymbol{\mu}) : \mathcal{D} \rightarrow \mathbb{R}$, $q = 1, \dots, Q_F$, are smooth functions, while $F^q : X \rightarrow \mathbb{R}$, $q = 1, \dots, Q_F$, are $\boldsymbol{\mu}$ -independent continuous linear functionals.

Let $X^\mathcal{N} \subset X$ be a conforming finite element space with \mathcal{N} degrees of freedom, we can now set the *truth* approximation of the problem (1):

$$(6) \quad \begin{aligned} &\text{find } u^\mathcal{N}(\boldsymbol{\mu}) \in X^\mathcal{N} \text{ s.t.} \\ &a(u^\mathcal{N}(\boldsymbol{\mu}), v^\mathcal{N}; \boldsymbol{\mu}) = F(v^\mathcal{N}; \boldsymbol{\mu}), \quad \forall v^\mathcal{N} \in X^\mathcal{N}. \end{aligned}$$

As we are considering the conforming FE case, conditions similar to (2) and (3) are fulfilled by restriction. More precisely, as regards the coercivity of the restriction of a to $X^\mathcal{N} \times X^\mathcal{N}$, we define:

$$(7) \quad \alpha^\mathcal{N}(\boldsymbol{\mu}) := \inf_{v^\mathcal{N} \in X^\mathcal{N}} \frac{a(v^\mathcal{N}, v^\mathcal{N}; \boldsymbol{\mu})}{\|v^\mathcal{N}\|_X^2}, \quad \forall \boldsymbol{\mu} \in \mathcal{D}$$

and, as we are considering a restriction, it easily follows that $\alpha(\boldsymbol{\mu}) \leq \alpha^\mathcal{N}(\boldsymbol{\mu})$, $\forall \boldsymbol{\mu} \in \mathcal{D}$. Similarly, for the continuity, we can define

$$(8) \quad +\infty > \gamma^\mathcal{N}(\boldsymbol{\mu}) = \sup_{v^\mathcal{N} \in X^\mathcal{N}} \sup_{w^\mathcal{N} \in X^\mathcal{N}} \frac{|a(v^\mathcal{N}, w^\mathcal{N}; \boldsymbol{\mu})|}{\|v^\mathcal{N}\|_X \|w^\mathcal{N}\|_X}, \quad \forall \boldsymbol{\mu} \in \mathcal{D}.$$

As we have already mentioned, also the domain of the equation can depend on the parameter. In this case we need to map the parametric domain $\Omega_p(\boldsymbol{\mu})$ onto a reference one denoted with Ω , via suitable parameter-dependent transformation $T(\cdot; \boldsymbol{\mu}) : \Omega \rightarrow \Omega_p(\boldsymbol{\mu})$, see [4, 20, 29, 33]. This allows to track back on the reference domain Ω all the involved bilinear and linear forms, so that (4) and (5) are defined on a common reference domain Ω . In this work we used only affine mappings [20, 33] that allow to easily recover the affinity assumptions (4) and (5). In [33, 43] it is possible to find, in particular, a detailed treatment of the advection–diffusion operators.

2.1.2. The reduced basis method: main features. Let us suppose that we are given a problem in the form (1) and its *truth* approximation (6). We recall that the dimension of the finite element space $X^\mathcal{N}$ is \mathcal{N} . Given an integer $N \ll \mathcal{N}$, suppose that we are given a set of N suitable parameter values, $S_N = \{\boldsymbol{\mu}^1, \dots, \boldsymbol{\mu}^N\}$: this allows us to define the *reduced basis space* as $X_N^\mathcal{N} = \text{span}\{u^\mathcal{N}(\boldsymbol{\mu}^n) : 1 \leq n \leq N\}$. To be more precise, a Gram-Schmidt orthonormalization

process on $\{u^{\mathcal{N}}(\boldsymbol{\mu}^n) : 1 \leq n \leq N\}$ is usually carried out for the sake of numerical stability, and the resulting orthonormal functions are considered as bases of the reduced space [20, 43].

Given a value $\boldsymbol{\mu} \in \mathcal{D}$ of the parameter we define the RB solution $u_N^{\mathcal{N}}(\boldsymbol{\mu})$ such that:

$$(9) \quad a(u_N^{\mathcal{N}}(\boldsymbol{\mu}), v_N; \boldsymbol{\mu}) = F(v_N; \boldsymbol{\mu}) \quad \forall v_N \in X_N^{\mathcal{N}}.$$

Recalling that $N \ll \mathcal{N}$, we emphasize the fact that to find the RB solution we need just to solve a $N \times N$ linear system, instead of the $\mathcal{N} \times \mathcal{N}$ one of the FE method.

The set S_N is built in the Offline stage, together with the particular solutions which span $X_N^{\mathcal{N}}$, using a Greedy algorithm [20, 43]. The latter chooses, at each step, the parameter value which maximizes a suitable a posteriori error estimator $\boldsymbol{\mu} \mapsto \Delta_N(\boldsymbol{\mu})$ such that

$$(10) \quad |||u^{\mathcal{N}}(\boldsymbol{\mu}) - u_N^{\mathcal{N}}(\boldsymbol{\mu})|||_{\boldsymbol{\mu}} \leq \Delta_N(\boldsymbol{\mu}) \quad \forall \boldsymbol{\mu} \in \mathcal{D},$$

where $|||\cdot|||_{\boldsymbol{\mu}}$ is the norm induced by the symmetric part of the bilinear form $a(\cdot, \cdot; \boldsymbol{\mu})$. The algorithm stops when a prescribed tolerance ε_{tol}^* is reached, that is when $\Delta_N(\boldsymbol{\mu}) \leq \varepsilon_{tol}^*$ for each parameter value $\boldsymbol{\mu}$ in a training set $\Xi_{train} \subset \mathcal{D}$. We assume in this section that Ξ_{train} is a collection of randomly selected parameter values according to an uniform distribution. The error estimator Δ_N has to be sharp, in order to avoid an unnecessarily high dimension N for the reduced basis space. Moreover, it must be computationally inexpensive in order to speed up the Greedy algorithm (within which it is computed many times) and to allow the certification of the RB solution during the *Online* stage. The estimator Δ_N is based on the residual and it requires the computation of a lower bound $\boldsymbol{\mu} \mapsto \alpha_{LB}(\boldsymbol{\mu})$ for the coercivity constant (2), which can be computed using the Successive Constraint Method (SCM) [22, 20].

We want to point out that all the expensive computations (i.e. those whose costs depend on the FE space dimension \mathcal{N}) are performed during the *Offline* stage. Indeed, the affinity assumptions (4) and (5) are crucial for the *Offline–Online* decoupling, as it is extensively shown in [20, 43]. The affinity assumptions allow the storage, during the *Offline* stage, of the matrices corresponding to the parameter independent forms $a_q, q = 1, \dots, Q_a$, restricted to $X_N^{\mathcal{N}}$. Thanks to this fact, during the *Online* stage the assembly of the reduced basis system only consists in a linear combination of these precomputed matrices. A similar strategy can also be applied to the computation of the error estimator [20, 43]. If these assumptions are not fulfilled, it turns out to be necessary an interpolation strategy (e.g. empirical interpolation method (EIM) [6, 15]) in order to recover them. A weighted version of EIM is provided in [10].

2.2. Stabilized reduced basis methods. The main goal of this section is to design an efficient stabilization procedure for the RB method. More specifically, we will make a comparison between an *Offline–Online* stabilized method and an *Offline–only* stabilized one as done in [37]. We want to approximate the solution of a parametric advection–diffusion problem:

$$(11) \quad -\varepsilon \Delta u + \boldsymbol{\beta} \cdot \nabla u = f \quad \text{in } \Omega \subset \mathbb{R}^d$$

given a parameter value $\boldsymbol{\mu} \in \mathcal{D}$ and suitable Dirichlet, Neumann or mixed boundary conditions. Here $\varepsilon = \varepsilon(\boldsymbol{\mu}) : \Omega \rightarrow [0, +\infty)$ is a parametrized diffusion coefficient, while $\boldsymbol{\beta} = \boldsymbol{\beta}(\boldsymbol{\mu}) : \Omega \rightarrow \mathbb{R}^d$ is a parametrized advection field such that $\text{div}(\boldsymbol{\beta}) = 0$.

Let \mathcal{T}_h be a triangulation of Ω and let K be an element of \mathcal{T}_h . We say that a problem is advection dominated in K if the following condition holds:

$$(12) \quad \mathbb{P}e_K(x) := \frac{|\boldsymbol{\beta}(x)|h_K}{2\varepsilon(x)} > 1 \quad \forall x \in K,$$

where h_K is the diameter of K . It is very well known from literature (e.g. [42]) that the FE approximation of advection dominated problems can show significant instability phenomena, e.g.

spurious oscillations near the boundary layers. Several recipes have been proposed to fix these issues. We choose to resort to a strongly consistent stabilization method: the Streamline/Upwind Petrov–Galerkin (SUPG) [7, 21, 27, 28]. For a detailed presentation of the stabilization method for the FE approximation of advection dominated problems, we refer to [42].

Let us now explain the basic ideas of the two RB stabilization methods mentioned before. As regards the *Offline–Online* stabilized method, the choice of the name reveals that the Galerkin projections are performed, in both *Offline* and *Online* stage, with respect to the SUPG stabilized bilinear form, that is

$$(13) \quad a_{stab}(w^{\mathcal{N}}, v^{\mathcal{N}}; \boldsymbol{\mu}) = a(w^{\mathcal{N}}, v^{\mathcal{N}}; \boldsymbol{\mu}) + s(w^{\mathcal{N}}, v^{\mathcal{N}}; \boldsymbol{\mu})$$

$$(14) \quad a(w^{\mathcal{N}}, v^{\mathcal{N}}; \boldsymbol{\mu}) = \int_{\Omega} \varepsilon(\boldsymbol{\mu}) \nabla w^{\mathcal{N}} \cdot \nabla v^{\mathcal{N}} + (\boldsymbol{\beta}(\boldsymbol{\mu}) \cdot \nabla w^{\mathcal{N}}) v^{\mathcal{N}}$$

$$(15) \quad s(w^{\mathcal{N}}, v^{\mathcal{N}}; \boldsymbol{\mu}) = \sum_{K \in \mathcal{T}_h} \delta_K \int_K L w^{\mathcal{N}} \frac{h_K}{|\boldsymbol{\beta}(\boldsymbol{\mu})|} L_S v^{\mathcal{N}}$$

where $w^{\mathcal{N}}, v^{\mathcal{N}}$ chosen in a suitable piecewise polynomial space $X^{\mathcal{N}}$. In (13) L is the parameter dependent advection–diffusion operator, that is $Lv^{\mathcal{N}} = \varepsilon \Delta v^{\mathcal{N}} + \boldsymbol{\beta} \cdot \nabla v^{\mathcal{N}}$, which can be split in its symmetric part $L_S u^{\mathcal{N}} = -\varepsilon \Delta u^{\mathcal{N}}$ and its skew–symmetric part $L_{SS} u^{\mathcal{N}} = \boldsymbol{\beta} \cdot \nabla u^{\mathcal{N}}$.

In contrast, in the *Offline–only* stabilized method we use the stabilized form (13) only during the *Offline* stage, while during the *Online* stage we project with respect to the standard advection–diffusion bilinear form (14). An advantage of using the *Offline–only* stabilized method would be a certain reduction of the online computational effort in the assembly of the reduced linear system, that could be also significant if the number of affine stabilization terms is very high. Among possible disadvantages, we mention the inconsistency between the offline and online bilinear forms.

We will start from the study of some test problems, which we will keep as prototypes for each further extension that will be carried out in the next sections. The first one is a **PG** problem [25, 40, 37], while the second is a parametrized internal layer problem [37]. From here on, we will explicitly write the FE space dimension \mathcal{N} only when it will be strictly necessary.

2.2.1. Numerical test: Poiseuille–Graetz problem (PG). We consider a **PG** problem where we have two parameters: one physical (the inverse of diffusivity coefficient μ_1 , which is proportional to the Péclet number) and one geometrical (the length of the domain being equal to $1 + \mu_2$). The **PG** problem deals with steady forced heat convection (advective phenomenon) combined with heat conduction (diffusive phenomenon) in a duct with walls at different temperature. Let us define $\boldsymbol{\mu} = (\mu_1, \mu_2)$ with both μ_1 and μ_2 positive, real numbers. Let $\Omega_p(\boldsymbol{\mu})$ be the rectangle $(0, 1 + \mu_2) \times (0, 1)$ in \mathbb{R}^2 . The domain is shown in figure 1. The problem is to find a solution $u(\boldsymbol{\mu})$,

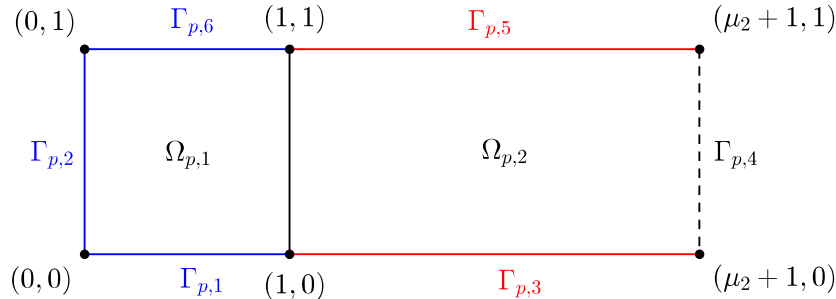


FIGURE 1. Geometry of **PG** problem. Parametrized domain. Boundary conditions: homogeneous Dirichlet on blue sides, $u = 1$ on red sides, homogeneous Neumann on the dashed side

representing the temperature distribution, such that:

$$(16) \quad \begin{cases} -\frac{1}{\mu_1} \Delta u(\boldsymbol{\mu}) + 4y(1-y) \partial_x u(\boldsymbol{\mu}) = 0 & \text{in } \Omega_p(\boldsymbol{\mu}) \\ u(\boldsymbol{\mu}) = 0 & \text{on } \Gamma_{p,1}(\boldsymbol{\mu}) \cup \Gamma_{p,2}(\boldsymbol{\mu}) \cup \Gamma_{p,6}(\boldsymbol{\mu}) \\ u(\boldsymbol{\mu}) = 1 & \text{on } \Gamma_{p,3}(\boldsymbol{\mu}) \cup \Gamma_{p,5}(\boldsymbol{\mu}) \\ \frac{\partial u}{\partial \nu} = 0 & \text{on } \Gamma_{p,4}(\boldsymbol{\mu}). \end{cases}$$

We set the reference domain as $\Omega = (0, 2) \times (0, 1)$, and subdivide it in $\Omega^1 = (0, 1) \times (0, 1)$ and $\Omega^2 = (1, 2) \times (0, 1)$. The affine transformation that maps the reference domain into the parametrized one is:

$$(17) \quad T^1(\boldsymbol{\mu}) : \Omega^1 \rightarrow \Omega_{p,1}(\boldsymbol{\mu}) \subset \mathbb{R}^2 \quad T^2(\boldsymbol{\mu}) : \Omega^2 \rightarrow \Omega_{p,2}(\boldsymbol{\mu}) \subset \mathbb{R}^2$$

$$(18) \quad T^1 \left(\begin{pmatrix} x \\ y \end{pmatrix}; \boldsymbol{\mu} \right) = \begin{pmatrix} x \\ y \end{pmatrix} \quad T^2 \left(\begin{pmatrix} x \\ y \end{pmatrix}; \boldsymbol{\mu} \right) = \begin{pmatrix} \mu_2 x \\ y \end{pmatrix} + \begin{pmatrix} 1 - \mu_2 \\ 0 \end{pmatrix}.$$

and define the continuous one-to-one transformation $T(\boldsymbol{\mu})$ by gluing together these two transformations.

Let us now define a mesh \mathcal{T}_h on the reference domain Ω and let us call \mathcal{T}_h^1 and \mathcal{T}_h^2 the restrictions \mathcal{T}_h to Ω_1 and Ω_2 , respectively. We use \mathbb{P}^1 FE discretization during the offline stage. Hence, the corresponding bilinear forms $a(\cdot, \cdot; \boldsymbol{\mu})$ and $s(\cdot, \cdot; \boldsymbol{\mu})$ are

$$(19) \quad \begin{aligned} a(u^\mathcal{N}, v^\mathcal{N}; \boldsymbol{\mu}) := & \int_{\Omega^1} \frac{1}{\mu_1} \nabla u^\mathcal{N} \nabla v^\mathcal{N} + 4y(1-y) \partial_x u^\mathcal{N} v^\mathcal{N} + \\ & + \int_{\Omega^2} \frac{1}{\mu_1 \mu_2} \partial_x u^\mathcal{N} \partial_x v^\mathcal{N} + \frac{\mu_2}{\mu_1} \partial_x u^\mathcal{N} \partial_y v^\mathcal{N} + 4\mu_2 y(1-y) \partial_x u^\mathcal{N} v^\mathcal{N} \end{aligned}$$

and

$$(20) \quad s(u^\mathcal{N}, v^\mathcal{N}; \boldsymbol{\mu}) := \sum_{K \in \mathcal{T}_h^1} h_K \int_K (4y(1-y) \partial_x u^\mathcal{N}) \partial_x v^\mathcal{N} + \sum_{K \in \mathcal{T}_h^2} \frac{h_K}{\sqrt{\mu_2}} \int_K (4y(1-y) \partial_x u^\mathcal{N}) \partial_x v^\mathcal{N}.$$

The choice of the stabilization coefficient $\delta_{K_p} = \delta_{K_p}(\boldsymbol{\mu}) = \frac{1}{\sqrt{\mu_2}}$ for $K_p \in \mathcal{T}_h^2$ is motivated by the transformation to the reference domain.

We test the performance of the RB approximation for two choices of the parameter space, namely $\mathcal{D}^1 = [10^4, 10^5] \times [0.5, 4]$ and $\mathcal{D}^2 = [1, 10^6] \times [0.5, 4]$. The parameter space \mathcal{D}^1 features very large values of μ_1 , so that the solution manifold is characterized by solution with steep boundary layers. In contrast, the parameter space \mathcal{D}^2 features both small and large values of μ_1 , resulting in a richer set of solutions. The range of variation for the geometrical parameter μ_2 is the same in both parameter spaces.

The comparison of *Offline-only* and *Offline-Online* stabilized algorithms is shown in figure 2, for \mathcal{D}^1 (left) and \mathcal{D}^2 (right). In each figure, the evolution of the greedy parameter selection is presented, plotting both the error bound $\Delta_N(\boldsymbol{\mu})$ employed by the RB algorithm and, for comparison, the exact energy norm error. For both \mathcal{D}^1 and \mathcal{D}^2 , the greedy algorithm in the *Online-Offline* case is clearly converging as the RB space enriches its dimension. In contrast, the greedy algorithm does not converge in the *Offline-only* case, being over 10^{-2} for both \mathcal{D}^1 and \mathcal{D}^2 .

We show a representative online solution for both stabilization cases, characterized by large value of Péclet number, in figure 3. As we can see, the *Offline-Online* stabilized RB solution is showing marked boundary layers, while the *Offline-only* stabilized RB solution still has some noise near the boundary layer and some peaks near discontinuities of solution at top and bottom walls.

Moreover, if we compare the time used to perform one $\mathcal{N} = 4369$ *true* solution and a RB one, we can see that the former lasts 0.6434561 seconds, while the latter lasts 0.0716783 seconds, on

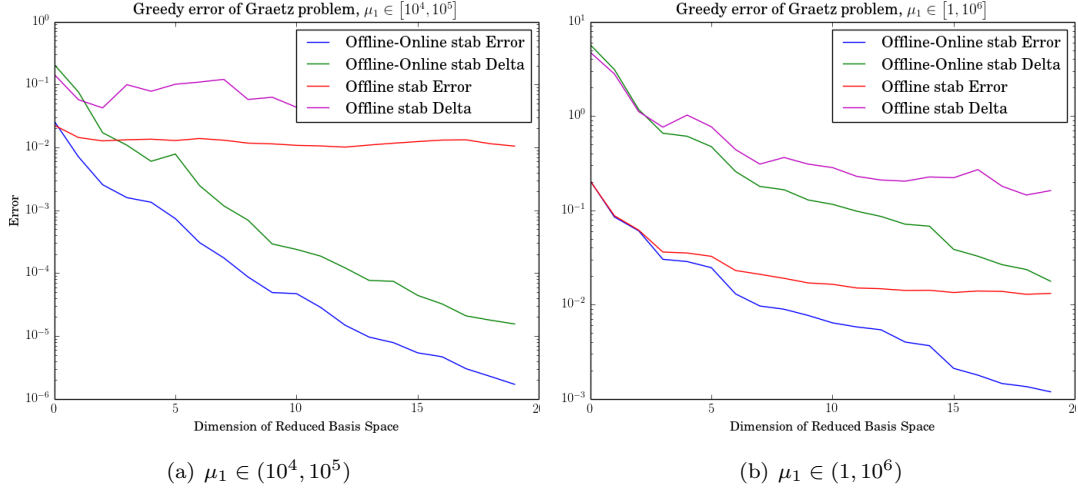
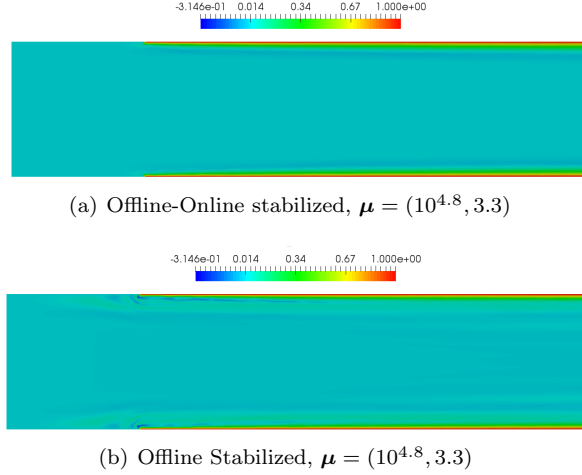


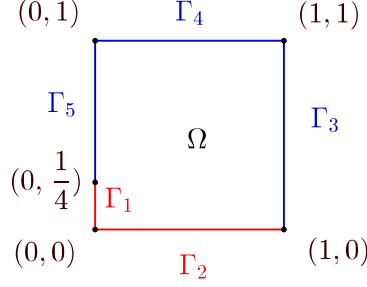
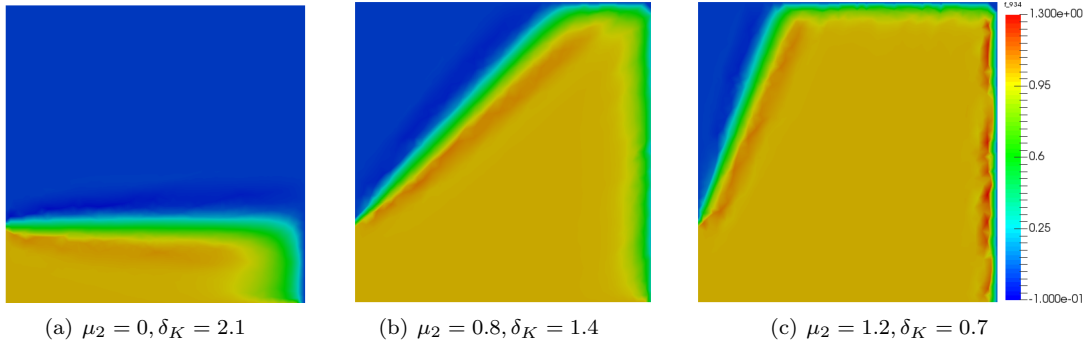
FIGURE 2. Error comparison between Offline and Online-Offline stabilization

average on a test set. This solution was performed for a $N = 20$ -dimension reduced basis space. We can even see bigger gains in parabolic section 4, where we save more computational time, with respect to the true solution.

FIGURE 3. RB solution, stabilized Offline-Online and Offline, $\mu = (10^{4.8}, 3.3)$

2.2.2. Numerical test: propagating front in a square (PFS). In this section we will test the reduced order stabilization method for a second test case where the parameter controls the angle of an internal layer. The problem we want to study is set over a unit square $\Omega \subset \mathbb{R}^2$, as sketched in figure 4, it has two parameter $\mu_1, \mu_2 \in \mathbb{R}$, and is as follows:

$$(21) \quad \begin{cases} -\frac{1}{\mu_1} \Delta u(\mu) + (\cos \mu_2, \sin \mu_2) \cdot \nabla u(\mu) = 0 & \text{in } \Omega \\ u(\mu) = 1 & \text{on } \Gamma_1 \cup \Gamma_2 \\ u(\mu) = 0 & \text{on } \Gamma_3 \cup \Gamma_4 \cup \Gamma_5. \end{cases}$$

FIGURE 4. Geometry **PFS** problemFIGURE 5. FE solution comparison varying δ_K and μ_2

Let us note that μ_1 is proportional to the Péclet number of the advection–diffusion problem, while μ_2 is the angle between the x axis and the direction of the constant advection field. The bilinear form associated to the problem is:

$$(22) \quad a(u, v; \boldsymbol{\mu}) = \int_{\Omega} \frac{1}{\mu_1} \nabla u \cdot \nabla v + (\cos \mu_2 \partial_x u + \sin \mu_2 \partial_y u) v.$$

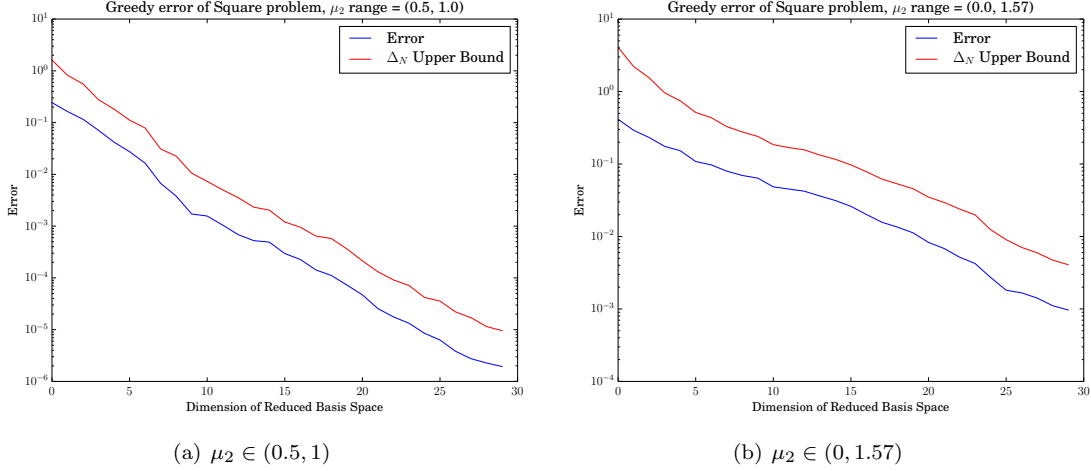
We introduce again a triangulation \mathcal{T}_h on the domain Ω and we consider a \mathbb{P}^1 discretization. The corresponding stabilization term is

$$(23) \quad s(u^{\mathcal{N}}, v^{\mathcal{N}}; \boldsymbol{\mu}) = \sum_{K \in \mathcal{T}^{\mathcal{N}}} \delta_K \int_K (\cos \mu_2, \sin \mu_2) \cdot \nabla u^{\mathcal{N}} (\cos \mu_2, \sin \mu_2) \cdot \nabla v^{\mathcal{N}}$$

where δ_K is manually tuned according to μ_2 . A few representative FE solutions are shown in figure 5. The figure clearly shows that the direction of the advection fields largely affects the solution, which exhibits strong variations in energy norm [36]. For this reason, we test the RB method for two different choices of the parameter space, namely $\mathcal{D}^1 = [10^4, 10^5] \times [0.5, 1]$ and $\mathcal{D}^2 = [10^4, 10^5] \times [0, 1.57]$. Both choices are characterized by dominant advection; moreover, a wider range of angles is considered in \mathcal{D}^2 than in \mathcal{D}^1 , resulting in a richer manifold of solutions.

The performance of the RB algorithm is shown in figure 6 for \mathcal{D}^1 (left) and \mathcal{D}^2 (left). Only the *Offline–Online* stabilization case is reported, since the *Offline-only* case gave poor results as in the previous test case. In both cases the stabilized reduced order method converges, reaching an error around 10^{-6} for \mathcal{D}^1 and around 10^{-3} for \mathcal{D}^2 .

Computational times are: 0.046551 seconds on average for a $\mathcal{N} = 309$ *true* solution and 0.0287261 seconds ($N = 20$) for a RB one. The gain is not enough to justify the RB in this test case, but we have to keep in mind that this was just a toy example to verify the validity of the method. For instance, we can see more significant improvements in parabolic section 4.

FIGURE 6. RB error and Δ_N error bound varying μ_2 range

3. Stabilized weighted reduced basis algorithm for problems with uncertain parameters. The reduced basis method formulated in section 2 assumed deterministic parameters; in contrast, for random parameters, a *weighted* reduced basis has been proposed [8, 9] as an extension of the standard reduced basis approach. The main idea of this method is to suitably assign a larger weight to those samples that are more “important”. In this section, we will deal with problems with random distributed parameters and we will compare the weighted method to the standard reduced basis method for advection–diffusion problems with high Péclet number. Moreover, we will also provide an offline/online stabilization approach that can be useful in case when stabilization involves large computations.

3.1. A brief introduction to weighted reduced basis method. To discuss the weighted reduced basis method [9], we introduce stochastic partial differential equations. Let Ω be an open set of \mathbb{R}^d with Lipschitz boundary $\partial\Omega$ and let $H_0^1(\Omega) \subset X \subset H^1(\Omega)$ a functional space. Let (A, \mathcal{F}, P) denote a complete probability space, where A is a set of outcomes $\omega \in A$, \mathcal{F} is a σ -algebra of events and $P : \mathcal{F} \rightarrow [0, 1]$ with $P(A) = 1$ is a probability measure [14]. A real-valued *random variable* is defined as a measurable function $Y : (A, \mathcal{F}) \rightarrow (\mathbb{R}, \mathcal{B})$, being \mathcal{B} the Borel σ -algebra on \mathbb{R} . Let $dF_Y(y)$ denote the distribution measure, i.e., for all $B \subset \mathcal{D}$, $P(F \in B) = \int_B dF_Y(y)$. Provided that $dF_Y(y)$ is absolutely continuous with respect to the Lebesgue measure dy , which we assume hereafter to be the case, there exists a probability density function $\rho : \mathcal{D} \rightarrow \mathbb{R}$ such that $\rho(y)dy = dF_Y(y)$. Note that the new measure space $(\mathcal{D}, \mathcal{B}(\mathcal{D}), \rho(y)dy)$ is isometric to (A, \mathcal{F}, P) under the random variable Y .

We define the probability Hilbert space $L^2(A) := \{v : A \rightarrow \mathbb{R} : \int_A v^2(\omega)dP(\omega) < \infty\}$ and $L_\rho^2(\mathcal{D}) := \{u : \mathcal{D} \rightarrow \mathbb{R} : \int_{\mathcal{D}} u^2(y)\rho(y)dy < \infty\}$, equipped with the equivalent norms (by noting that $v(\omega) = u(y(\omega))$)

$$(24) \quad \|v\|_{L^2(A)} := \left(\int_A v^2(\omega)dP(\omega) \right)^{1/2} = \left(\int_{\mathcal{D}} u^2(y)\rho(y)dy \right)^{1/2} =: \|u\|_{L_\rho^2(\mathcal{D})}.$$

Let $v : \Omega \times A \rightarrow \mathbb{R}$ be a real-valued *random field*, which is a real-valued random variable defined on A for each $x \in \Omega$. We define the Hilbert space $S(\Omega) := L^2(A) \otimes H^1(\Omega)$, equipped with the inner product

$$(25) \quad (u, v) = \int_A \int_\Omega (uv + \nabla u \cdot \nabla v) \, dx \, dP(\omega) \quad \forall u, v \in S(\Omega),$$

where ∇ is the spatial gradient in Ω . The associated norm is defined as $\|v\|_{S(\Omega)} = \sqrt{(v, v)}$.

Now we can introduce *stochastic partial differential equations*. Given random vector field $\boldsymbol{\mu} : A \rightarrow \mathbb{R}^p$, our stochastic advection-diffusion problem will be finding a random field $u(x; \boldsymbol{\mu}(\omega))$ such that

$$(26) \quad -\varepsilon(\boldsymbol{\mu}(\omega))\Delta u(\boldsymbol{\mu}(\omega)) + \boldsymbol{\beta}(\boldsymbol{\mu}(\omega)) \cdot \nabla u(\boldsymbol{\mu}(\omega)) = f(\boldsymbol{\mu}(\omega)) \quad \text{in } \Omega(\boldsymbol{\mu}(\omega)),$$

accompanied by suitable boundary conditions.

Now, we want to develop an algorithm that gives more importance to parameters with higher probability of been chosen. The basic idea is to assign different weights to every values of parameter $\boldsymbol{\mu} \in \mathcal{D} \subset \mathbb{R}^p$ according to a prescribed weight function $w(\boldsymbol{\mu}) > 0$, and to use them during the procedure of construction of the RB space. The motivation is that when the parameter $\boldsymbol{\mu}$ has non constant weight function $w(\boldsymbol{\mu})$, e.g. stochastic problems with random inputs obeying probability distribution far from uniform type, the weighted approach can considerably attenuate the computational effort for large scale computational problems. The weighted reduced basis method consists of the same elements, namely greedy algorithm, a posteriori error estimate and *Offline-Online* decomposition, as presented in section 2.1. In this section, we only highlight the new weighted steps.

Let $X^\mathcal{N}$ be a high-fidelity approximation space of X , equipped with the previously defined norm $\|u(\boldsymbol{\mu})\|_\mu \forall u \in X$ at some reference value $\tilde{\boldsymbol{\mu}} \in \mathcal{D}$. Moreover, let us define an equivalent weighted norm

$$(27) \quad \|u(\boldsymbol{\mu})\|_w = w(\boldsymbol{\mu})\|u(\boldsymbol{\mu})\|_\mu \quad \forall u \in X^\mathcal{N}, \forall \boldsymbol{\mu} \in \mathcal{D},$$

where $w : \mathcal{D} \rightarrow \mathbb{R}^+$ is a weighted function taking positive real values, which we assume to be continuous and bounded. We will denote by X_w the space X endowed with $\|\cdot\|_w$.

The greedy algorithm is thus modified to take the weighting into account, that is to solve an optimization problem in $L^\infty(\mathcal{D}; X_w)$: at each step we are seeking a new parameter $\boldsymbol{\mu}^N \in \mathcal{D}$ such that

$$(28) \quad \boldsymbol{\mu}^N = \arg \sup_{\boldsymbol{\mu} \in \Xi_{train}} \|u^\mathcal{N}(\boldsymbol{\mu}) - u_N(\boldsymbol{\mu})\|_w,$$

where again u_N is the reduced basis approximation of the *truth* solution $u^\mathcal{N}$. Here, Ξ_{train} is the discretized version of the parameter space \mathcal{D} . Instead of performing the true error, we use a weighted *a posteriori* error estimator Δ_N^w such that

$$(29) \quad \|u^\mathcal{N}(\boldsymbol{\mu}) - u_N(\boldsymbol{\mu})\|_w \leq \Delta_N^w(\boldsymbol{\mu}).$$

The choice of the weight function $w(\boldsymbol{\mu})$ is aimed by the desire of minimizing the squared norm error of the RB approximation in the space $L^\infty(\mathcal{D}; X_w)$, i.e.

$$(30) \quad \begin{aligned} \mathbb{E}[\|u^\mathcal{N} - u_N\|^2] &= \int_A \int_\Omega \|u^\mathcal{N}(\boldsymbol{\mu}(\omega)) - u_N(\boldsymbol{\mu}(\omega))\|_\mu^2 dx dP(\omega) = \\ &= \int_{\mathcal{D}} \int_\Omega \|u^\mathcal{N}(\boldsymbol{\mu}) - u_N(\boldsymbol{\mu})\|_\mu^2 \rho(\boldsymbol{\mu}) dx d\boldsymbol{\mu}, \end{aligned}$$

that we can bound with

$$(31) \quad \mathbb{E}[\|u^\mathcal{N} - u_N\|^2] \leq \int_{\mathcal{D}} \Delta_N(\boldsymbol{\mu})^2 \rho(\boldsymbol{\mu}) d\boldsymbol{\mu},$$

where Δ_N is the RB error estimator introduced in section 2.1. This motivates us in the choice $w(\boldsymbol{\mu}) = \sqrt{\rho(\boldsymbol{\mu})}$. Finally, we set $\Delta_N^w(\boldsymbol{\mu}) := \Delta_N(\boldsymbol{\mu})\sqrt{\rho(\boldsymbol{\mu})}$ [9].

Another important aspect in the RB algorithm is the choice of the training set Ξ_{train} . While in the deterministic case we used Uniform Monte Carlo sampling methods to choose elements from \mathcal{D} , in the stochastic context we can use a Monte Carlo sampling according to the distribution $\rho(\boldsymbol{\mu})$. We will see in numerical test that this choice is important to improve the convergence of the error. We refer to [8, 9, 11] for further details on weighted reduced basis methods.

3.2. Stabilized weighted reduced basis methods. In this section we study a variant of the weighted reduced basis method suited for stochastic advection–diffusion equations with high Péclet number. In order to do so, we combine the stabilization of advective terms, introduced in section 2, to the weighting procedure of section 3.1.

As in section 2, for the moment, we need to add SUPG stabilization terms to the weak form of the problem. This results in the following formulation:

$$(32) \quad \begin{aligned} &\text{find } u^{\mathcal{N}}(\boldsymbol{\mu}(\omega)) \in X^{\mathcal{N}} \text{ s.t.} \\ &a_{stab}(u^{\mathcal{N}}(\boldsymbol{\mu}(\omega)), v^{\mathcal{N}}; \boldsymbol{\mu}(\omega)) = F_{stab}(v^{\mathcal{N}}; \boldsymbol{\mu}(\omega)) \quad v^{\mathcal{N}} \in X^{\mathcal{N}}, \forall \omega \in A, \end{aligned}$$

where a_{stab} and F_{stab} are defined in section 2. The most relevant difference with respect to the previous section is that $\boldsymbol{\mu} : A \rightarrow \mathcal{D}$ is a random vector, instead of being a deterministic parameter.

We test the proposed method with stochastic versions of the previous test cases (**PG** problem 2.2.1 and **PFS** problem 2.2.2). In order to do so, we need to prescribe the distribution of $\boldsymbol{\mu}$; this will be done for each test case in the following sections.

3.2.1. Numerical test: Poiseuille–Graetz problem. For **PG** problem, we consider the range $\mathcal{D} = [10^1, 10^6] \times [0.5, 4]$ for the parameter $\boldsymbol{\mu}$. To give more importance to parameter with $\mu_1 \approx 10^5$, we use $X_1 \sim \text{Beta}(4, 2)$ and $\mu_1 \sim 10^{1+5 \cdot X_1}$, while $X_2 \sim \text{Beta}(3, 4)$ and $\mu_2 \sim 0.5 + 3.5X_2$. We choose the Beta distribution because it takes values in a compact set, resulting in $(\mu_1, \mu_2) \in \mathcal{D}$.

We compare next the performance of the reduction method for the different choices that we have discussed in section 3, namely related to using weighted or standard greedy algorithm, and the sampling of the training set Ξ_{train} . We present in figure 7 numerical results for four different cases:

1. Classical Greedy with Uniform Monte Carlo sampling (black line);
2. Classical Greedy with Beta Monte Carlo sampling (purple line);
3. Weighted Greedy with Uniform Monte Carlo sampling (green line);
4. Weighted Greedy with Beta Monte Carlo sampling (red line).

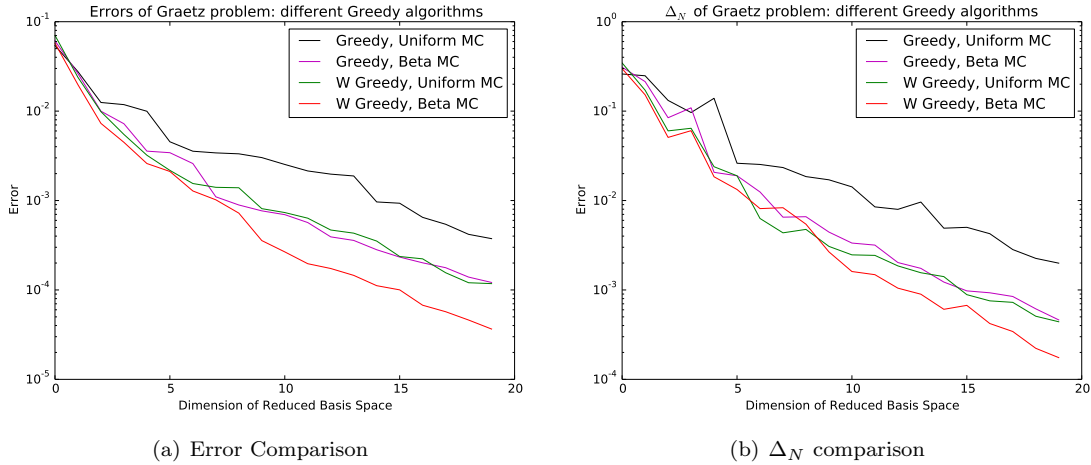


FIGURE 7. Greedy algorithms comparison for Graetz problem

We used 200 samples for Ξ_{train} in each algorithm during the offline stage. We can see in figure 7 the comparison between the average errors and the average Δ_N between these algorithms for a test set of size 100, with the same distribution as the training set. The results show that both weighting and a correct sampling are essential to obtain the best convergence results [46]. Indeed,

putting together these two aspects we get the best results, reaching an error that is one tenth of the error of the classical Greedy algorithm on uniform distribution.

In a similar way, instead of computing the average of the errors on the test set, we can also compute the mean of the error in a probability sense, i.e.

$$(33) \quad \mathbb{E}[\|u^{\mathcal{N}}(\boldsymbol{\mu}) - u_N(\boldsymbol{\mu})\|_{\boldsymbol{\mu}}] = \int_{\mathcal{D}} \|u^{\mathcal{N}}(\boldsymbol{\mu}) - u_N(\boldsymbol{\mu})\|_{\boldsymbol{\mu}} \rho(\boldsymbol{\mu}) d\boldsymbol{\mu},$$

that we can approximate using some quadrature method. In particular, we will use Monte Carlo method, i.e.

$$(34) \quad \mathbb{E}[\|u^{\mathcal{N}}(\boldsymbol{\mu}) - u_N(\boldsymbol{\mu})\|_{\boldsymbol{\mu}}] \approx \frac{1}{M} \sum_{i=1}^M \|u^{\mathcal{N}}(\boldsymbol{\mu}_i) - u_N(\boldsymbol{\mu}_i)\|_{\boldsymbol{\mu}_i} \rho(\boldsymbol{\mu}_i),$$

where $\boldsymbol{\mu}_i$, $i = 1, \dots, M$ are randomly chosen parameters in the testing test. Results are nevertheless similar to the ones presented in figure 7, and the same conclusions can be drawn. For instance, the probabilistic mean of the errors in the classical Greedy method with uniform sampling and the weighted reduced one with Beta sampling are $4.5485 \cdot 10^{-4}$ and $1.2807 \cdot 10^{-4}$, respectively.

3.2.2. Numerical test: propagating front in a square. We can proceed in the same way for the **PFS** problem of section 2.2.2. In this section, the parameter range \mathcal{D} is $[10^4, 10^5] \times [0, 1.5]$. Also in this case μ_1 and μ_2 depend on randomly distributed Beta variables, i.e. $\mu_1 \sim 10^4 + 9 \cdot 10^4 \cdot X_1$ and $\mu_2 \sim 1.5 \cdot X_2$, where $X_1 \sim \text{Beta}(3, 4)$ while $X_2 \sim \text{Beta}(4, 2)$.

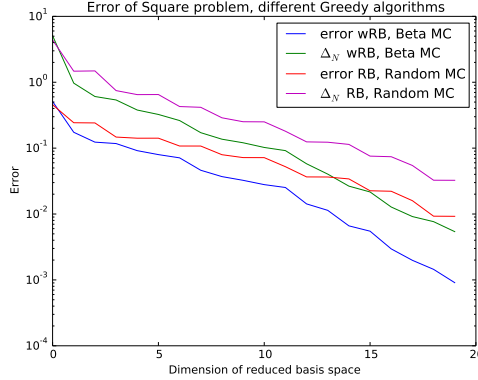


FIGURE 8. Greedy algorithms comparison for **PFS** problem

As for the previous test case we compare the classical Greedy method with Uniform Monte Carlo to the weighted reduced basis method with Beta Monte Carlo distribution. The comparison, shown in figure 8, provides results which are very similar to **PG** problem. Indeed, the weighted RB method with Beta distribution is converging faster than the classical one. Also the mean errors in the probabilistic sense of (34) show a similar behavior: for a reduced basis space of dimension $N = 20$, the stabilized weighted method with Beta distribution produces a mean error of $1.7803 \cdot 10^{-3}$, while the classical approach gives a mean error of $7.9362 \cdot 10^{-3}$.

3.3. Selective online stabilization of weighted reduced basis approach. In this section we want to optimize computational costs in the *Online* phase of RB method. Indeed, stabilization procedure can lead to an increase in the number Q_a and/or Q_f of affine terms, which in turn may lead to larger online times required for the assembly of the linear system or for the evaluation of the error estimator. In this section we propose a procedure to selectively enable online stabilization only when required.

3.3.1. Numerical test: Poiseuille–Graetz problem. Let us consider first the **PG** example, with Beta distribution over parameter μ , similarly to section 3.2.1. In what follows, we assume that $\mu_1 \in [10, 10^6]$, $\mu_1 \sim 10^{1+5 \cdot X_1}$ where $X_1 \sim \text{Beta}(5, 3)$. To simplify the discussion of the results we further assume that $\mu_2 \equiv 1$.

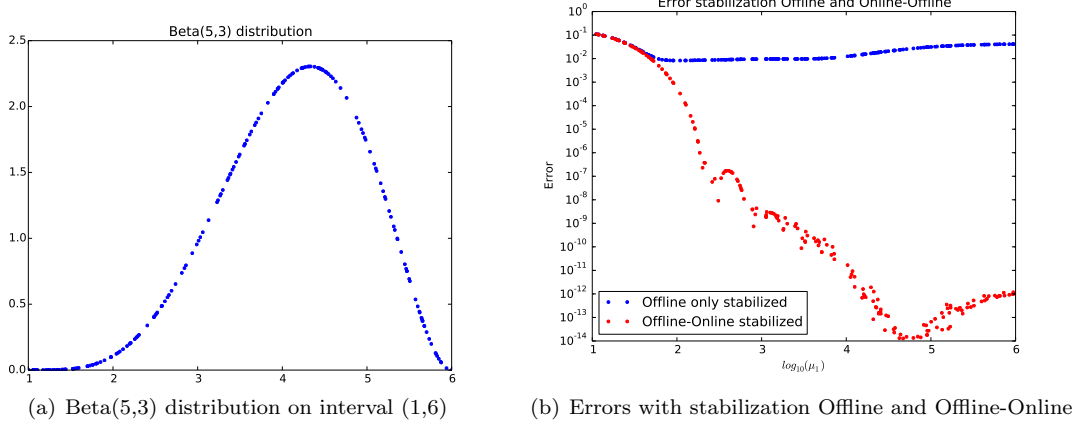


FIGURE 9. Error and density of Uniform Monte Carlo test set

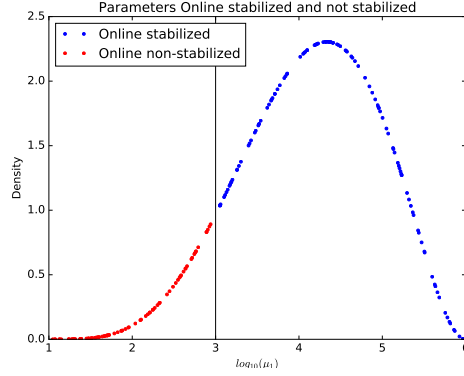
While carrying out the online stage of the proposed stabilized weighted reduced basis method, we can choose whether to apply online stabilization or not. Figure 9(b) shows the resulting error on a test set (that we have taken with a Uniform Monte Carlo sampling), sorted by increasing values of μ_1 , considering both options. We can observe that for low Péclet number ($\mu_1 \leq 10^2$), *Offline-Online* stabilization and *Offline only* stabilization produce very similar results. Thus, we would prefer the less expensive *Offline only* stabilization procedure. Moreover, in the regions where the density of μ is very small, even a large error would be less relevant in terms of the probabilistic mean error (33). So, we should consider the idea of enabling the more expensive online stabilization only for parameters with high density (which would affect more the mean error) or parameters with large Péclet numbers (were the more expensive assembly is fully justified by the convection dominated regime).

Let us start considering the case where we want to stabilize *Online* solutions depending on Péclet numbers. First, we establish a threshold at a certain Péclet number $\tilde{\mu}_1$. For parameters $\mu_1 > \tilde{\mu}_1$ we will use both *Online* and *Offline* stabilization, while for parameter $\mu_1 \leq \tilde{\mu}_1$ we will use only *Offline* stabilization. See figure 10 for a graphical representation for $\tilde{\mu}_1 = 10^3$. For different thresholds $\tilde{\mu}_1$ we can compute the error in sense of (33), as we can see in the following table.

Threshold $\tilde{\mu}_1$	Error	Percentage non-stabilized
10^1	$7.9673 \cdot 10^{-4}$	0%
$10^{1.5}$	$8.0704 \cdot 10^{-4}$	10%
10^2	$10.0060 \cdot 10^{-4}$	20%
$10^{2.5}$	$18.2806 \cdot 10^{-4}$	33%
10^3	$33.4593 \cdot 10^{-4}$	45%
10^6	0.021128	100%

Considering that the best attainable error was of $7.967 \cdot 10^{-4}$, we can say that until $\tilde{\mu}_1 = 10^2$ we are not worsening considerably the error (less than an order of magnitude). At the same time, we can save online time on the assembly of terms related to stabilization coefficient for 20% of our test set (that was uniformly distributed).

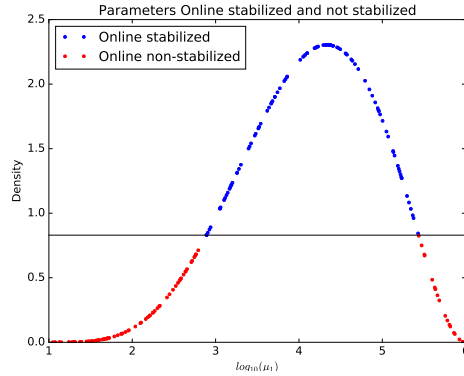
The other natural gauge to decide whether to stabilize *Online*, or not, is the density $\rho(\mu)$. Let

FIGURE 10. *Péclet discriminant, black line is the Péclet threshold*

$\tilde{\nu}$ be a prescribed tolerance; we will not stabilize parameters μ on the tail I of the distribution such that

$$(35) \quad \int_I \rho(\mu) d\mu = \tilde{\nu},$$

where I is a set $\{\mu : \rho(\mu) \leq \tilde{\rho}\}$ for some suitable $\tilde{\rho}$ which can be easily found numerically as a function of $\tilde{\nu}$. In figure 11 we can see an example for $\tilde{\nu} = 10\%$.

FIGURE 11. *Density discriminant, black line is the density threshold*

In the following table, we summarize some results for different thresholds $\tilde{\nu}$ (and, correspondingly, $\tilde{\rho}$).

Threshold $\tilde{\nu}$	Threshold $\tilde{\rho}$	Error	Percentage non-stabilized
0	0	$7.9673 \cdot 10^{-4}$	0%
0.001	0.02233	$9.3222 \cdot 10^{-4}$	15%
0.002	0.04423	$9.6456 \cdot 10^{-4}$	17%
0.005	0.09094	$14.7861 \cdot 10^{-4}$	21%
0.01	0.13877	$15.9482 \cdot 10^{-4}$	25%
0.02	0.21433	$25.6017 \cdot 10^{-4}$	30%
0.05	0.38244	$49.1931 \cdot 10^{-4}$	38%
0.1	0.89068	$66.7488 \cdot 10^{-4}$	45%
1	∞	0.021128	100%

We have that errors computed using density discriminant are less accurate than ones computed with Péclet discriminant. Indeed, for the same percentage of non-stabilized solution (for example 45%) we have bigger errors in density discriminant approach ($66 \cdot 10^{-4}$ instead of $33 \cdot 10^{-4}$). This is due to the enormous difference between *Online* stabilized and *Online* non-stabilized solution for high Péclet numbers (figure 9(b)), with the latter resulting in considerably larger errors.

3.3.2. Numerical test: propagating front in a square. Let us now consider the **PFS** problem with fixed $\mu_1 \equiv 10^5$, while $\mu_2 \sim 0.5 + 3.5X_2 \in [0, 1.5]$ where $X_2 \sim \text{Beta}(4, 2)$. We have decided to fix the Péclet number since results in section 2.2.2 show that the solution is most sensible to the parameter μ_2 , which represents the angle of the propagating front.

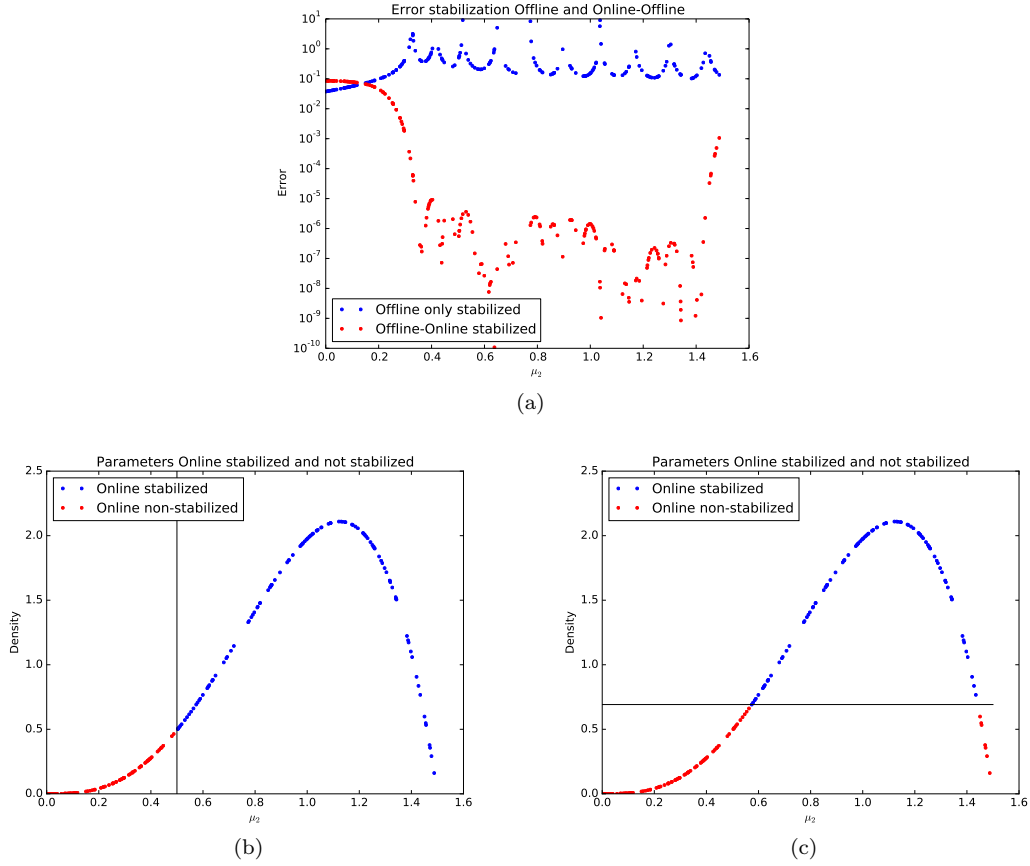


FIGURE 12. (a) Errors with stabilization Offline and Offline-Online; (b) angle discriminant, black line is the angle threshold; (c) density discriminant, black line is the density threshold

Errors for *Online* stabilized and *Online* not stabilized solutions over a Uniform Monte Carlo test set of 200 elements are provided in figure 12(a), for increasing values of μ_2 . We can notice that *Offline-Online* stabilized errors of solutions with small angles (figure 12(a), $\mu_2 \lesssim 0.2$) are bigger than *Offline-only* stabilized errors. This is due to the fact that the density of that region of the parameter range is very small and thus the weighted greedy algorithm picks very few parameters in that region. In a similar way, we also notice that solutions for $\mu_2 \approx 1.5$ are not well approximated. Indeed, in the *Offline only* stabilized case the lack of stabilization is badly affecting the reduced order solution for any $\mu_2 \gtrsim 0.2$, while in the *Offline-Online* stabilized case the low density of $\mu_2 \gtrsim 1.4$ leads the weighted reduced basis selection to choose few parameters $\mu_2 \approx 1.5$ during the offline stage.

Thus, in a similar way to the previous test case, we propose selective online stabilization criteria, either depending on a threshold on the parameter (the angle μ_2 in this case, rather than the Péclet number) or on the probability distribution. Let us start from a discussion of the former choice, leading to online stabilize for angles greater than a certain threshold $\tilde{\mu}_2$ (see e.g. figure 12(b)). The error for different thresholds $\tilde{\mu}_2$ is tabulated as follows:

Threshold $\tilde{\mu}_2$	Error	Percentage non-stabilized
0	0.01416	0%
0.1	0.01400	6%
0.2	0.01506	16%
0.3	0.04056	23%
0.4	0.11810	30%
0.5	0.20365	37%
1.5	0.82998	100%

We can observe that at the beginning the error is decreasing as the threshold increases, while it slowly increases after a critical angle between 0.1 and 0.2. Due to this, we consider a threshold $\tilde{\mu}_2 = 0.2$ to be optimal in order not to increase the error and save 16% of online stabilization computations.

As for **PG** example, we can also test a criterion based on a density threshold (see e.g. figure 12(c)). In the following table, we are showing different errors for different density thresholds.

Threshold $\tilde{\nu}$	Threshold $\tilde{\rho}$	Error	Percentage non-stabilized
0	0	0.01416	0%
0.001	0.02271	0.01400	13%
0.002	0.04600	0.01506	16%
0.005	0.10237	0.02269	20%
0.01	0.13598	0.04658	25%
0.02	0.26309	0.11158	30%
0.05	0.51855	0.20613	38%
0.1	0.72557	0.32034	46%
1	∞	0.82998	100%

In this case, a negligible increase of the error is obtained for $\tilde{\nu} = 0.002$, allowing to save more than 15% of stabilized *Online* computations. Further computational savings can be obtained for $\tilde{\nu} = 0.01$, up to 25%, at the expense of a larger error. We notice that in this case both criteria give similar results: this is due to the fact that errors are large for both *Offline only* and *Offline-Online* stabilization methods when μ_2 is large or where density ρ is small.

Remark 3.1. Let I be the region of the parameter space where *Offline only* stabilized solution is selected, and let $\mathcal{D} \setminus I$ denote the complement region in which the *Offline-Online* stabilized method is queried. Let $u_N^I(\boldsymbol{\mu})$ denote the corresponding reduced order solution for $\boldsymbol{\mu} \in I$, and similarly $u_N^{\mathcal{D} \setminus I}(\boldsymbol{\mu})$ for $\boldsymbol{\mu} \in \mathcal{D} \setminus I$. To ease the notation, we will denote the online solution by $u_N(\boldsymbol{\mu})$ when no confusion arises.

The selective procedure for online stabilization can be automatically tuned according to a prescribed tolerance on the probabilistic mean error $\mathbb{E} [\|u^N(\boldsymbol{\mu}) - u_N(\boldsymbol{\mu})\|_{\boldsymbol{\mu}}]$. In order to estimate the mean error, we recall the standard error estimation (10) for $\boldsymbol{\mu} \in \mathcal{D} \setminus I$, and the following error estimation

$$(36) \quad \begin{aligned} \|u_N^I(\boldsymbol{\mu}) - u^N(\boldsymbol{\mu})\|_{\boldsymbol{\mu}} &\leq \Delta_N^I(\boldsymbol{\mu}) := h_{max}(\boldsymbol{\mu})C(\boldsymbol{\mu})\|\boldsymbol{\beta} \cdot \nabla u^N(\boldsymbol{\mu})\|_{L^2(\Omega_p(\boldsymbol{\mu}))} + \\ &\quad + (1 + h_{max}(\boldsymbol{\mu})C(\boldsymbol{\mu})^2\|\boldsymbol{\beta}\|_{L^\infty(\Omega_p(\boldsymbol{\mu}))})\varepsilon^*. \end{aligned}$$

for $\boldsymbol{\mu} \in I$ [37], where $C(\boldsymbol{\mu})$ is the constant of the equivalence between H^1 and $\|\cdot\|_{\boldsymbol{\mu}}$ norms, h_{max} is the maximum mesh size, while ε^* is the tolerance of the greedy algorithm [37].

Thus, combining these two error estimators, we get that

$$(37) \quad \mathbb{E} [\|u^{\mathcal{N}}(\boldsymbol{\mu}) - u_N\|_{\boldsymbol{\mu}}] \leq (1 - \tilde{\nu}) \max_{\boldsymbol{\mu} \in \mathcal{D} \setminus I} \Delta_N(\boldsymbol{\mu}) + \tilde{\nu} \max_{\boldsymbol{\mu} \in I} \Delta_N^I(\boldsymbol{\mu}).$$

which, for a given tolerance \tilde{e} on the mean error, allows us to compute $\tilde{\nu}$ such that

$$(1 - \tilde{\nu}) \max_{\boldsymbol{\mu} \in \mathcal{D} \setminus I} \Delta_N(\boldsymbol{\mu}) + \tilde{\nu} \max_{\boldsymbol{\mu} \in I} \Delta_N^I(\boldsymbol{\mu}) < \tilde{e}.$$

Remark 3.2. We remark that this selective approach for online stabilization is peculiar of stochastic problems. Indeed, it is the density distribution and the relative importance of each sample in the computation of the probabilistic mean that drives the selection process. Such a weighting is lacking in a deterministic setting, being all samples equally probable during the online stage.

4. Stabilized weighted reduced basis method for stochastic parabolic equations. In this section we extend our investigation to stochastic time dependent advection–diffusion equations. Stabilization of advection diffusion parabolic equations with high Péclet number have been studied in several works with different stabilization methods [7]. We will adapt SUPG stabilization for FE methods on parabolic equations to RB method, as suggested in [36, 37, 38, 39]. The reduction will employ a POD-Greedy procedure [19, 35, 40] during the offline stage.

Like for stochastic elliptic equations, we define a *parameter domain* \mathcal{D} as a closed subset of \mathbb{R}^p and we call $\boldsymbol{\mu}$ a random field with values in \mathcal{D} . Again, let Ω be a bounded open subset of \mathbb{R}^d ($d = 1, 2, 3$) with regular boundary $\partial\Omega$ and let X be a functional space such that $H_0^1(\Omega) \subset X \subset H^1(\Omega)$. For each outcome $\omega \in A$, and corresponding realization $\boldsymbol{\mu}(\omega) \in \mathcal{D}$, we define the continuous and coercive bilinear forms a and m such that satisfy the *affinity* assumption like (4) and a linear form F which satisfies the *affine* assumption (5). Let us finally denote the time domain as $I = [0, T]$, where T is the final time.

We can now define the weak form of the continuous stochastic problem:

$$(38) \quad \begin{aligned} &\text{find } u(t; \boldsymbol{\mu}(\omega)) \in X, \quad \forall t \in I, \quad \forall \omega \in A, \quad \text{continuous in } t \text{ s.t.} \\ &m(\partial_t u(t; \boldsymbol{\mu}(\omega)), v) + a(u(t; \boldsymbol{\mu}(\omega)), v; \boldsymbol{\mu}(\omega)) = g(t)F(v; \boldsymbol{\mu}(\omega)) \quad \forall v \in X, \quad \forall t \in I, \quad \forall \omega \in A \\ &\text{given the initial value } u(0; \boldsymbol{\mu}(\omega)) = u_0 \in L^2(\Omega) \end{aligned}$$

where $g : I \rightarrow \mathbb{R}$ is a *control function* such that $g \in L^2(I)$. We choose a right hand side of the form $g(t)F(v; \boldsymbol{\mu})$, as usual in the RB framework [18, 40], in order to ease the *Offline–Online* computational decoupling.

4.1. Discretization and RB formulation. To discretize the time–dependent problem (38) we follow the approach used in [18, 20, 34, 40], that is to use finite differences in time and FE in space discretization [41]. We start by discretizing the spatial part of the problem (resulting in a mesh denoted by \mathcal{T}_h) and the temporal part (resulting in discrete time steps $\{t_j = j \cdot \Delta t\}_{j=0}^J$). We thus define the FE *truth* approximation space $X^{\mathcal{N}}$ and we denote its basis with $\{\phi_i\}_{i=1}^{\mathcal{N}}$. The fully *discretized* problem reads

$$(39) \quad \begin{aligned} &\text{for each } 1 \leq j \leq J, \text{ find } u_j^{\mathcal{N}}(\boldsymbol{\mu}(\omega)) \in X^{\mathcal{N}} \text{ s.t.} \\ &\frac{1}{\Delta t} m(u_j^{\mathcal{N}}(\boldsymbol{\mu}(\omega)) - u_{j-1}^{\mathcal{N}}(\boldsymbol{\mu}(\omega)), v^{\mathcal{N}}; \boldsymbol{\mu}(\omega)) + a(u_j^{\mathcal{N}}(\boldsymbol{\mu}(\omega)), v^{\mathcal{N}}; \boldsymbol{\mu}(\omega)) = \\ &g(t_j)F(v^{\mathcal{N}}; \boldsymbol{\mu}(\omega)) \quad \forall v^{\mathcal{N}} \in X^{\mathcal{N}}, \quad \forall \omega \in A, \\ &\text{given the initial condition } u_0^{\mathcal{N}} \text{ s.t.} \\ &(u_0^{\mathcal{N}}, v^{\mathcal{N}})_{L^2(\Omega)} = (u_0, v^{\mathcal{N}})_{L^2(\Omega)} \quad \forall v^{\mathcal{N}} \in X^{\mathcal{N}}. \end{aligned}$$

The latter problem uses the *Backward Euler–Galerkin* discretization, but we can resort to other theta-methods (e.g. Crank–Nicholson) or to high order method (e.g. Runge–Kutta) [41].

The RB formulation of the problem (39) is based on hierarchical RB space, as we did for the steady case, employing a POD reduction over the time trajectory and a greedy selection over the parameter space [19, 35].

In particular, the algorithm first finds the parameter μ^* for which the whole time evolution of the solution $(u_j^\mathcal{N}(\mu^*))_{1 \leq j \leq J}$ is the worst approximated in the RB space with a Greedy algorithm. Then, it carries out a projection of this solution of a chosen parameter onto the orthogonal of the reduced basis space RB^\perp , in order not to consider information already taken into account. Furthermore it compresses the resulting space by a POD method and finally it orthonormalizes them thanks to respect to the previous bases with a Gram–Schmidt algorithm.

For the *a posteriori* error estimates, we follow the choice presented in [18]. The RB formulation of the problem can be obtained by substituting the reduced basis space $X_N^\mathcal{N}$ to $X^\mathcal{N}$ in (39).

4.2. SUPG stabilization method for parabolic problems. In this section we briefly introduce the SUPG method for time-dependent problems [7, 28]. The idea is the same of the steady case: we have to add terms to bilinear forms in order to improve stability. The stabilization term is almost the same than in the steady case, but now we have to consider also the time dependency to guarantee the strong consistency. We thus set

$$(40) \quad s(w^\mathcal{N}(t), v^\mathcal{N}) = \sum_{K \in \mathcal{T}_h} \delta_K \left(\partial_t w^\mathcal{N}(t) + Lw^\mathcal{N}(t), \frac{h_K}{|\beta(\mu(\omega))|} L_{SS} v^\mathcal{N} \right)_K$$

where $w^\mathcal{N}(t) \in X^\mathcal{N}$ for each $t \in I$, $v^\mathcal{N} \in X^\mathcal{N}$ and $(\cdot, \cdot)_K$ is the usual L^2 scalar product, restricted to the element K . Here L is the steady advection–diffusion operator and L_{SS} is its skew–symmetric part.

Thus, we can define the *Backward Euler–SUPG* formulation of the problem by substituting the forms m , a and F in (39) with:

$$(41) \quad \begin{aligned} m_{stab}(w^\mathcal{N}, v^\mathcal{N}; \mu(\omega)) &= m(w^\mathcal{N}, v^\mathcal{N}; \mu(\omega)) + \sum_{K \in \mathcal{T}_h} \delta_K \left(w^\mathcal{N}, \frac{h_K}{|\beta(\mu(\omega))|} L_{SS} v^\mathcal{N} \right)_K \\ a_{stab}(w^\mathcal{N}, v^\mathcal{N}; \mu(\omega)) &= a(w^\mathcal{N}, v^\mathcal{N}; \mu(\omega)) + \sum_{K \in \mathcal{T}_h} \delta_K \left(Lw^\mathcal{N}, \frac{h_K}{|\beta(\mu(\omega))|} L_{SS} v^\mathcal{N} \right)_K \\ F_{stab}(v^\mathcal{N}; \mu(\omega)) &= F(v^\mathcal{N}; \mu(\omega)) + \sum_{K \in \mathcal{T}_h} \delta_K \left(f, \frac{h_K}{|\beta(\mu(\omega))|} L_{SS} v^\mathcal{N} \right)_K \end{aligned}$$

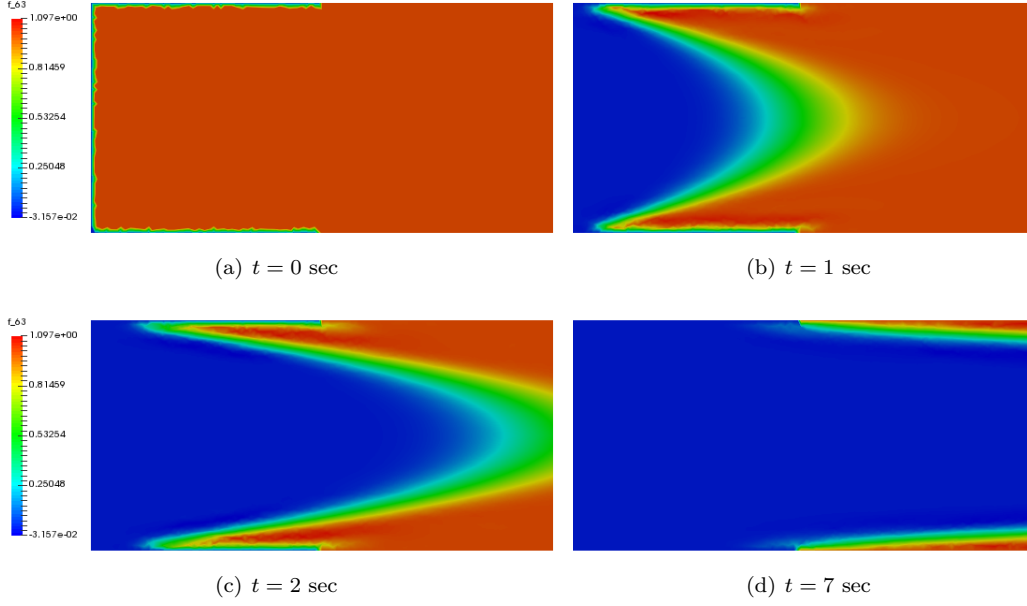
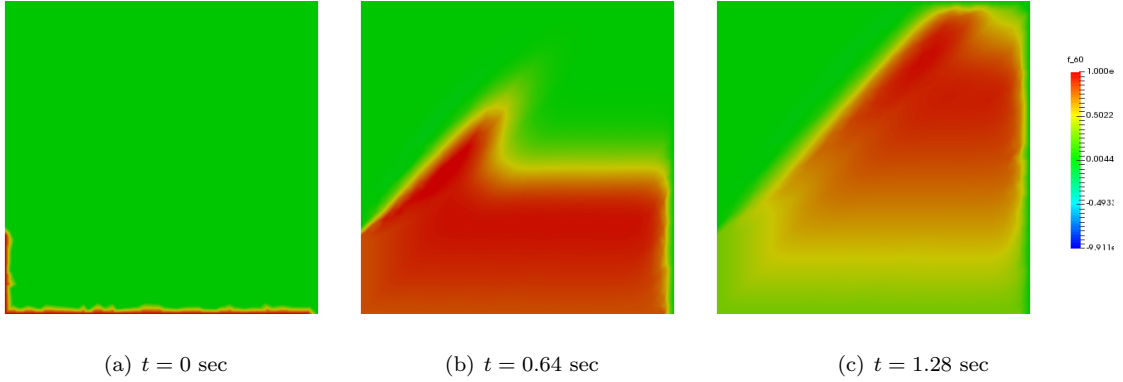
where K are the elements which form the mesh \mathcal{T}_h and f can be a source term of the advection–diffusion equation or a lifting of the Dirichlet boundary data. For the analysis of stability and convergence of the method we refer to [26].

4.3. Numerical tests for stochastic parabolic problems. We are now showing some numerical results of the stabilized RB method for stochastic parabolic PDEs, extending to the time dependent case the problems in sections 3.2.1 and 3.2.2. Few representative FE solutions are provided in figure 13 for the parabolic **PG** problem and figure 14 for the parabolic front propagation test.

We show in figure 16 the average of the error on a test set, for both the parabolic **PG** problem (left) and the parabolic front propagation test (right). The norm of the error is defined as

$$(42) \quad |||e^\mathcal{N}(\mu)|||_\mu = \left(m(e_J^\mathcal{N}(\mu), e_J^\mathcal{N}(\mu); \mu) + \sum_{j=1}^J a(e_j^\mathcal{N}(\mu), e_j^\mathcal{N}(\mu); \mu) \Delta t \right)^{\frac{1}{2}},$$

while the error estimator Δ_N is as in [18]. We compare in figure 16 the classical reduced basis algorithm (with uniform Monte Carlo sampling) and the weighted reduced basis one (with sampling

FIGURE 13. Plot of FE solution for parabolic **PG** problem at different times at $\mu_1 = 1$ and $\mu_2 = 1 \cdot 10^4$ FIGURE 14. Plot of FE solution for parabolic **PFS** problem at different times, $\mu_1 = 2 \cdot 10^4$, $\mu_2 = 0.8$

according to the distribution of $\boldsymbol{\mu}$). The comparison shows that, also for parabolic problem, proper weighting and suitable sampling allows to improve the accuracy of the resulting reduced order model (especially in the case of the parabolic front problem) and the reliability of the error estimator (in both test cases).

Similar results hold for the probabilistic mean indicator introduced in (33), which we extend to the unsteady case as

$$(43) \quad \mathbb{E}[||\mathbf{u}^{\mathcal{N}} - \mathbf{u}_N^{\mathcal{N}}||^2] := \sum_{j=1}^J \int_{\mathcal{D}} ||u_j^{\mathcal{N}}(\boldsymbol{\mu}) - u_{N,j}^{\mathcal{N}}(\boldsymbol{\mu})||_{\boldsymbol{\mu}}^2 \rho(\boldsymbol{\mu}) d\boldsymbol{\mu}$$

and approximate with Monte Carlo quadrature procedure. By doing this we obtain for **PG** problem with a reduced basis space of dimension 20 an error of $8.3248 \cdot 10^{-2}$ for classic Greedy algorithm and $7.6318 \cdot 10^{-2}$ for weighted reduced basis algorithm, respectively. For **PFS** problem we have

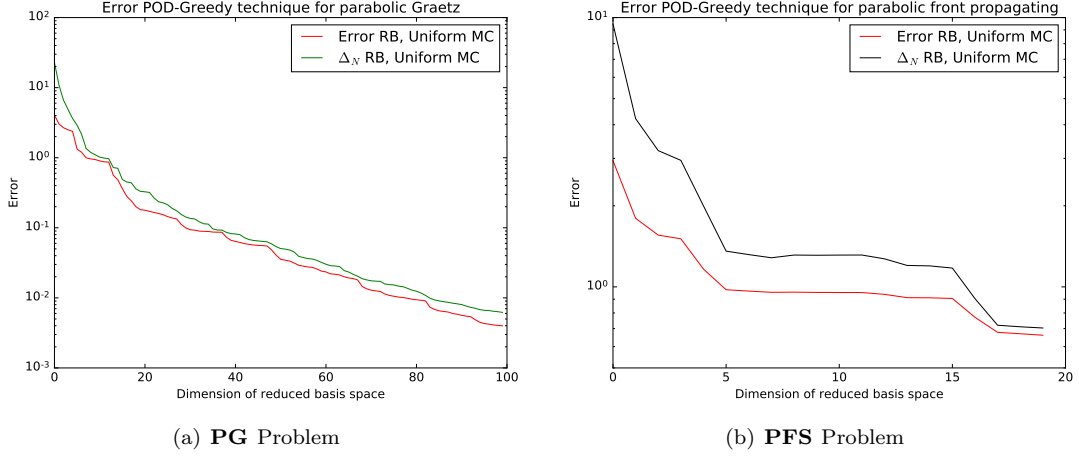


FIGURE 15. Greedy algorithms comparison for parabolic problems

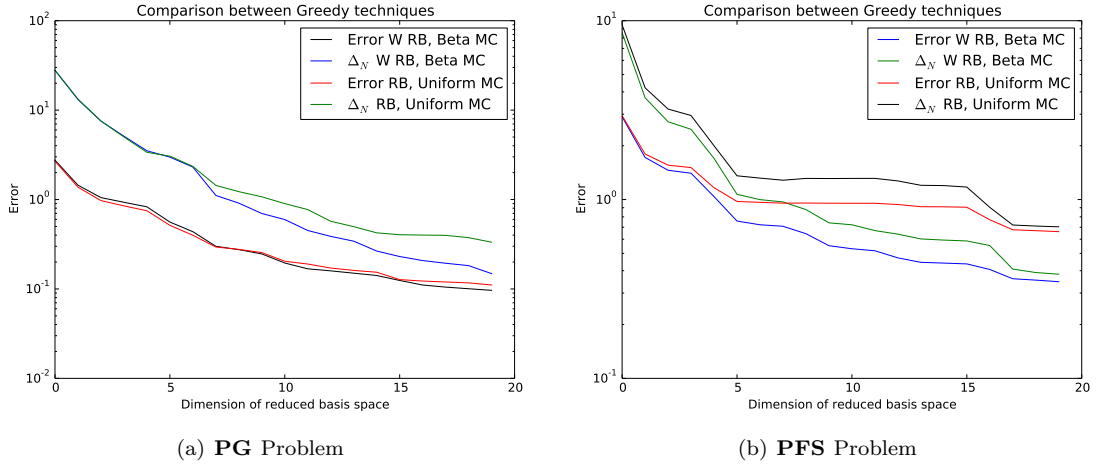


FIGURE 16. Greedy algorithms comparison for parabolic problems

that the classic Greedy algorithm produce an error of 0.3196 while the weighted algorithm gets 0.2343.

A small remark on computational times in parabolic must be done. In **PG** problem for one true parabolic solution we need 132.382 seconds, while for the RB one with $N = 20$ basis functions we need only 0.356224 seconds. For a **PFS** true solution we need 17.2846 seconds and only 0.125266 seconds for RB solution with $N = 20$ basis functions. These results justify all the computational costs of the *Offline* phase.

5. Conclusions. In this work we have dealt with stabilization techniques for the approximation of advection dominated problems using a reduced basis approach into a stochastic framework, both in steady and unsteady case. To perform a stabilization in the reduced basis algorithm, we have studied the SUPG [42] stabilization for FE method and introduced two reduced basis stabilization algorithms. The *Online-Offline* stabilization, which uses SUPG stabilized forms in both stages (*Offline* and *Online*) and the *Offline-only* stabilization, which uses the original (not stabi-

lized) forms for the *Online* stage. The underlying idea was to obtain a stable RB approximation, from the stable FE approximation, with reasonable computational times and, at the same time, a very good accuracy.

We then introduced stochastic equations and weighted reduced basis method [9]. We formulated a stabilized weighted reduced basis method for advection-diffusion problems with random input parameters. Numerical test cases clearly highlight the importance of the weighting procedure, as well as the necessity of a proper sampling of the parameter space, according to the probability distribution of μ . Moreover, we introduced a procedure to selectively enable online stabilization when required. This allows to reduce the number of terms to be assembled in the affine expansion, with a negligible worsening of the error, which remains of the same order as the one for the previous strategies.

Finally, we have generalized these methods to parabolic problems producing a stabilized RB approach for unsteady cases [19, 37], starting from SUPG stabilized parabolic FE methods [7, 28].

Possible further developments of this topic could be the application of these methods to more complex geometries, e.g. non-affinely parametrized ones, requiring some empirical interpolation preprocessing [6, 29]. Moreover, the method could be tested on larger dimension parameter spaces \mathcal{D} , using Monte Carlo or quasi-Monte Carlo strategies and on other types of probability distributions.

Acknowledgments. We acknowledge the support by European Union Funding for Research and Innovation – Horizon 2020 Program – in the framework of European Research Council Executive Agency: H2020 ERC Consolidator Grant 2015 AROMA-CFD project 681447 “Advanced Reduced Order Methods with Applications in Computational Fluid Dynamics”. We also acknowledge the INDAM-GNCS projects “Metodi numerici avanzati combinati con tecniche di riduzione computazionale per PDEs parametrizzate e applicazioni” and “Numerical methods for model order reduction of PDEs”. The computations in this work have been performed with RBniCS [5] library, developed at SISSA mathLab, which is an implementation in FEniCS [30] of several reduced order modelling techniques; we acknowledge developers and contributors to both libraries.

REFERENCES

- [1] I. AKHTAR, A. H. NAYFEH, AND C. J. RIBBENS, *On the stability and extension of reduced-order Galerkin models in incompressible flows*, Theoretical and Computational Fluid Dynamics, 23 (2009), pp. 213–237.
- [2] S. ALI, F. BALLARIN, AND G. ROZZA, *Stabilized reduced basis methods for parametrized Stokes and Navier-Stokes equations*. Submitted, 2017.
- [3] J. BAIGES, R. CODINA, AND S. IDELSOHN, *Explicit reduced-order models for the stabilized finite element approximation of the incompressible Navier–Stokes equations*, International Journal for Numerical Methods in Fluids, 72 (2013), pp. 1219–1243.
- [4] F. BALLARIN, E. FAGGIANO, S. IPPOLITO, A. MANZONI, A. QUARTERONI, G. ROZZA, AND R. SCROFANI, *Fast simulations of patient-specific haemodynamics of coronary artery bypass grafts based on a POD–Galerkin method and a vascular shape parametrization*, Journal of Computational Physics, 315 (2016), pp. 609–628.
- [5] F. BALLARIN, A. SARTORI, AND G. ROZZA, *RBniCS - reduced order modelling in FEniCS*. <http://mathlab.sissa.it/rbnics>, 2015.
- [6] M. BARRAULT, Y. MADAY, N. NGUYEN, AND A. PATERA, *An ‘empirical interpolation’ method: application to efficient reduced-basis discretization of partial differential equations*, C. R. Math. Acad. Sci., 339 (2004), pp. 667–672.
- [7] A. BROOKS AND T. HUGHES, *Streamline upwind/Petrov-Galerkin formulations for convection dominated flows with particular emphasis on the incompressible Navier-Stokes equations*, Comput. Methods Appl. Mech. Engrg., 32 (1982), pp. 199–259.
- [8] P. CHEN, *Model Order Reduction Techniques for Uncertainty Quantification Problems*, PhD thesis, École Polytechnique Fédérale de Lausanne EPFL, 2014, http://www.infoscience.epfl.ch/record/198689/files/EPFL_TH6118.pdf.
- [9] P. CHEN, A. QUARTERONI, AND G. ROZZA, *A weighted reduced basis method for elliptic partial differential equations with random input data*, SIAM Journal on Numerical Analysis, 51 (2013), pp. 3163–3185.
- [10] P. CHEN, A. QUARTERONI, AND G. ROZZA, *A weighted empirical interpolation method: a priori convergence analysis and applications*, ESAIM: Mathematical Modelling and Numerical Analysis, 48 (2014), pp. 943–953.

- [11] P. CHEN, A. QUARTERONI, AND G. ROZZA, *Reduced basis methods for uncertainty quantification*, SIAM/ASA Journal on Uncertainty Quantification, 5 (2017), pp. 813–869, <https://doi.org/10.1137/151004550>, <https://doi.org/10.1137/151004550>, <https://arxiv.org/abs/https://doi.org/10.1137/151004550>.
- [12] L. DEDÈ, *Reduced basis method for parametrized elliptic advection-reaction problems*, J. Comput. Math., 28 (2010), pp. 122–148.
- [13] E. DELGADO ÁVILA, T. CHACÓN REBOLLO, M. GÓMEZ-MÁRMOL, F. BALLARIN, AND G. ROZZA, *On a certified Smagorinsky reduced basis turbulence model*. In press, SIAM Journal on Numerical Analysis, 2017.
- [14] R. DURRETT, *Probability Theory and Examples*, Cambridge University Press, Cambridge, UK, 2010.
- [15] J. EFTANG, M. GREPL, AND A. PATERA, *A posteriori error bounds for the empirical interpolation method*, C. R. Math. Acad. Sci., 51 (2010), pp. 28–58.
- [16] F. GELSOMINO AND G. ROZZA, *Comparison and combination of reduced-order modelling techniques in 3D parametrized heat transfer problems*, Math. Comput. Model. Dyn. Syst., 17 (2011), pp. 371–394.
- [17] S. GIERE, T. ILIESCU, V. JOHN, AND D. WELLS, *Supg reduced order models for convection-dominated convection–diffusion–reaction equations*, Computer Methods in Applied Mechanics and Engineering, 289 (2015), pp. 454–474.
- [18] M. GREPL AND A. PATERA, *A Posteriori error bounds for reduced-basis approximations of parametrized parabolic partial differential equations*, M2AN Math. Model. Numer. Anal., 1 (2005), pp. 157–181.
- [19] B. HAASDONK AND M. OHLBERGER, *Reduced basis method for finite volume approximations of parametrized linear evolution equations*, ESAIM: M2AN, 42 (2008), pp. 277–302.
- [20] J. HESTHAVEN, G. ROZZA, AND B. STAMM, *Certified Reduced Basis Methods for Parametrized Partial Differential Equations*, Springer, 2016.
- [21] T. HUGHES AND A. BROOKS, *A multidimensional upwind scheme with no crosswind diffusion*, in Finite element methods for convection dominated flows, vol. 34, Am. Soc. Mech. Engrs, New York, 1979, pp. 19–35.
- [22] D. HUYNH, G. ROZZA, S. SEN, AND A. PATERA, *A successive constraint linear optimization method for lower bounds of parametric coercivity and inf-sup stability constants*, C. R. Math. Acad. Sci., 345 (2007), pp. 473–478.
- [23] T. ILIESCU, H. LIU, AND X. XIE, *Regularized reduced order models for a stochastic Burgers equation*. Submitted, <https://arxiv.org/abs/1701.01155>, 2017.
- [24] T. ILIESCU AND Z. WANG, *Variational multiscale proper orthogonal decomposition: Navier-Stokes equations*, Numerical Methods for Partial Differential Equations, 30 (2014), pp. 641–663.
- [25] F. INCROPERA AND D. DEWITT, *Fundamental of Heat and Mass Transfer*, John Wiley & Sons, 1990.
- [26] V. JOHN AND J. NOVO, *Error analysis of the SUPG finite element discretization of evolutionary convection–diffusion–reaction equations*, SIAM J. Numer. Anal., 49 (2011), pp. 1149–1176.
- [27] C. JOHNSON AND U. NÄVERT, *An analysis of some finite element methods for advection-diffusion problems*, in Analytical and numerical approaches to asymptotic problems in analysis (Proc. Conf., Univ. Nijmegen, Nijmegen, 1980), vol. 47 of North-Holland Math. Stud., North-Holland, Amsterdam, 1981, pp. 99–116.
- [28] C. JOHNSON, U. NÄVERT, AND J. PITKÄRANTA, *Finite element methods for linear hyperbolic problems*, Comput. Methods Appl. Mech. Engrg., 45 (1984).
- [29] T. LASSILA AND G. ROZZA, *Parametric free-form shape design with PDE models and reduced basis method*, Comput. Methods Appl. Mech. Engrg., 199 (2010), pp. 1583–1592.
- [30] A. LOGG, K. MARDAL, AND G. WELLS, *Automated Solution of Differential Equations by the Finite Element Method*, Springer-Verlag, Berlin, 2012.
- [31] S. LORENZI, A. CAMMI, L. LUZZI, AND G. ROZZA, *POD-Galerkin method for finite volume approximation of Navier–Stokes and RANS equations*, Computer Methods in Applied Mechanics and Engineering, 311 (2016), pp. 151–179.
- [32] Y. MADAY, A. MANZONI, AND A. QUARTERONI, *An online intrinsic stabilization strategy for the reduced basis approximation of parametrized advection-dominated problems*, tech. report, MATHISCE, 2016.
- [33] A. MANZONI, A. QUARTERONI, AND G. ROZZA, *Model reduction techniques for fast blood flow simulation in parametrized geometries*, Int. J. Numer. Meth. Biomed. Engrg., 28 (2012), pp. 604–625.
- [34] N. C. NGUYEN, G. ROZZA, D. B. P. HUYNH, AND A. T. PATERA, *Reduced Basis Approximation and a Posteriori Error Estimation for Parametrized Parabolic PDEs: Application to Real-Time Bayesian Parameter Estimation*, John Wiley & Sons, Ltd, 2010, pp. 151–177.
- [35] N.-C. NGUYEN, G. ROZZA, AND A. T. PATERA, *Reduced basis approximation and a posteriori error estimation for the time-dependent viscous burgers’ equation*, Calcolo, 46 (2009), pp. 157–185.
- [36] P. PACCARINI, *Stabilized reduced basis method for parametrized advection-diffusion PDEs*, master’s thesis, Università degli Studi di Pavia, 2012.
- [37] P. PACCARINI AND G. ROZZA, *Stabilized reduced basis method for parametrized advection–diffusion PDEs*, Comput. Methods Appl. Mech. Engrg., 274 (2014), pp. 1–18.
- [38] P. PACCARINI AND G. ROZZA, *Stabilized reduced basis method for parametrized scalar advection-diffusion problems at higher Péclet number: roles of the boundary layers and inner fronts*, in Proceedings of the jointly organized 11th World Congress on Computational Mechanics - WCCM XI, 5th European Congress on Computational Mechanics - ECCM V, 6th European Congress on Computational Fluid Dynamics - ECFD V, 2014, pp. 5614–5624.
- [39] P. PACCARINI AND G. ROZZA, *Reduced basis approximation of parametrized advection-diffusion PDEs with*

- high Péclet number*, in Numerical Mathematics and Advanced Applications - ENUMATH 2013: Proceedings of ENUMATH 2013, the 10th European Conference on Numerical Mathematics and Advanced Applications, Lausanne, August 2013, vol. 103, 2015, pp. 419–426.
- [40] A. QUARTERONI, G. ROZZA, AND A. MANZONI, *Certified reduced basis approximation for parametrized partial differential equations and applications*, J. Math. Ind., 1 (2011), pp. 1–44.
 - [41] A. QUARTERONI, R. SACCO, AND F. SALERI, *Numerical mathematics*, vol. 37 of Texts in Applied Mathematics, Springer-Verlag, Berlin, 2007.
 - [42] A. QUARTERONI AND A. VALLI, *Numerical Approximation of Partial Differential Equations*, Springer, 1994.
 - [43] G. ROZZA, D. HUYNH, AND A. PATERA, *Reduced basis approximation and a posteriori error estimation for affinely parametrized elliptic coercive partial differential equations: application to transport and continuum mechanics*, Arch. Comput. Methods Eng., 3 (2008), pp. 229–275.
 - [44] G. ROZZA, N. NGUYEN, A. PATERA, AND S. DEPARIS, *Reduced basis methods and a posteriori error estimators for heat transfer problems*, in ASME -American Society of Mechanical Engineers - Heat Transfer Summer Conference Proceedings, S. Francisco, CA, USA, 2009.
 - [45] G. STABILE, S. HIJAZI, A. MOLA, S. LORENZI, AND G. ROZZA, *Advances in reduced order modelling for CFD: vortex shedding around a circular cylinder using a POD-Galerkin method*. In press, <https://arxiv.org/abs/1701.03424>, CAIM, Communication in Applied and Industrial Mathematics, 2017.
 - [46] L. VENTURI, *Weighted reduced basis methods for parametrized PDEs in uncertainty quantification problems*, master’s thesis, Università degli Studi di Trieste / SISSA, Trieste, Italia, 2016.